The Microwave Spectrum of Imidazole; Complete Structure and the Electron Distribution from Nuclear Quadrupole Coupling Tensors and Dipole Moment Orientation

Dines Christen*, John H. Griffiths, and John Sheridan

School of Physical and Molecular Sciences, University College of North Wales, Bangor LL57 2UW, Gwynedd, U.K.

Z. Naturforsch. **37a**, 1378–1385 (1982); received November 8, 1981

Spectra have been measured for eleven isotopic forms of imidazole, including single substitutions at each nucleus in turn. A complete r_s-structure is obtained. The ring structure is:

N(1)–C(2) = 1.364 Å, C(2)–N(3) = 1.314 Å, N(3)–C(4) = 1.382 Å, C(4)–C(5) = 1.364 Å, C(5)–N(1) = 1.377 Å, ∢N(1)C(2)N(3) = 112.0°, ∢C(2)N(3)C(4) = 104.9°, ∢N(3)C(4)C(5) = 110.7°, ∢C(4)C(5)N(1) = 105.5° and ∢C(5)N(1)C(2) = 106.9°.

The N(1)–H(1) distance is 0.998 Å, while the C–H distances are all very close to 1.078 Å. The bonds N(1)–H(1) and C(2)–H(2) lie close to the external bisectors of the respective ring angles, but C(4)–H(4) and C(5)–H(5) are each displaced by several degrees from these bisectors towards N(3) and N(1) respectively. The electric dipole moment is established as 3.67 (5) D from Stark effects, directed almost parallel with the line joining the nitrogen nuclei. The properties and orientations of the two ^{14}N-nuclear quadrupole tensors have been investigated, in particular through the spectra of the two mono-^{14}N-imidazoles.

I. Introduction

The present work is part of a series of microwave studies of structures of heterocyclic five-membered rings [1]. Imidazole, NH—CH=N—CH=CH, is perhaps a specially interesting member of this family on account of the occurrence of its ring in biological structures. Knowledge of the gas-phase structure of imidazole is also desirable for comparison with results of studies of this molecule in the crystalline or dissolved states, in which, as in pyrazole [2], intermolecular hydrogen bonding can considerably modify the structure and indeed produce for some purposes a "pseudo-equivalence" of the two nitrogen positions, which microwave studies of both these substances show to be absent in the vapour.

A brief preliminary account of early stages of these studies has been given [1].

II. Experimental

Imidazole (Koch-Light) was recrystallized from benzene and, as in the case of all samples, sublimed in vacuum before use. Spectra of all the mono-^{13}C-imidazoles were measured in their natural concentrations. Samples containing some 20% of each of the mono-^{15}N-imidazoles were made by condensation [3] of ammonia (30 atom% ^{15}N) with glyoxal and formaldehyde. Deuterated imidazoles were made by exchange with D_2O under various conditions; 1-deuteroimidazole was prepared in high yield by exchange at room temperature; about a 90% yield of 1,2-dideuteroimidazole was made following published procedures [4] by treating imidazole with NaOD in D_2O at 60 °C; a mixture of 4-deutero-, 5-deutero-, and 4,5-dideuteroimidazole was obtained by heating imidazole with D_2O in a bomb at 250 °C for 4 hours, the 1- and 2-positions being finally reprotonated by treatment with H_2O **.

Spectra were measured with a conventional spectrometer with 100 kHz Stark-effect modulation. Free-running klystrons were used as sources, with oscilloscope display of spectra, except where nuclear hyperfine structures were analysed, where the sources were phase-locked and spectra recorded with slow sweeping. The low volatility of imidazole called for special sample-handling routines. Early measurements were made with the temperature of

* Present address: Institut für Physikalische Chemie der Universität Tübingen, D-7400 Tübingen, Auf der Morgenstelle 8.

Reprint requests to Dr. D. Christen, Institut für Physikalische Chemie der Universität Tübingen, D-7400 Tübingen, Auf der Morgenstelle 8.

** A sample of 2-deuteroimidazole was kindly provided by Professor J. H. Ridd.

0340-4811 / 81 / 1200-1378 $ 01.00/0. — Please order a reprint rather than making your own copy.

the sample and cell raised somewhat above room temperature. Better spectra, with less background of ammonia lines, were later obtained with cell-temperatures near 20 °C and use of a flowed sample, although for each isotopic form a considerable time was needed to "saturate" the cell with the species concerned. The measured frequencies are believed accurate to ± 0.1 MHz.

Many of the lines showed nuclear quadrupole hyperfine structure, the analysis of which (Sect. IV below) was taken into account in the listing of the unperturbed transition frequencies. When only the strongest component of the hyperfine pattern could be accurately measured, appropriate corrections were applied.

III. Analysis of Rotational and Centrifugal Distortion Constants

As in other cases of molecules close to the oblate symmetric-top limit, the spectral details varied in large and internally consistent ways with isotopic substitution. The large isotopic rotations of principal axes lead to corresponding changes in dipole components and quadrupole coupling constants. In particular, this behaviour prevents the preferred procedure of selecting equivalent transitions of every species to derive constants for structure calculations. The data used in such calculations, however, were selected as consistently as possible.

Table 1 summarizes the numbers of measured lines used in the analysis, for each isotopic species, with classification into a- and b-type and Q-and R-type transitions, and ranges of J-values. The dipole components are seen to vary in ways consistent with the overall dipole direction (Section VI). Full listings of the measured line-frequencies can be obtained from the authors, and have been deposited with the Sektion für Strukturdokumentation, University of Ulm, West Germany. We summarize the results of the analysis here in Table 2; in this, the rotational and distortion constants for the planar molecule case (with τ^*_{aabb} fixed at zero) were fitted to the measurements by least squares*. The numbers in parenthesis indicate two standard errors in the last numbers quoted for each constant. For 2-^{13}C-imidazole, R-branch transitions were not measured, and the constants tabulated were calculated with assumption of the inertial defect to be that of the parent. The data for 1,2-dideutero-imidazole did not justify such a detailed analysis;

Table 1. Numbers and types of rotational lines measured for different isotopic species of imidazole.

Molecule	Number	a-type	b-type	Q-type	R-type	J_{max}
Parent	80	57	23	75	5	38
1 D	29	29	0	23	6	34
2 D	36	0	36	31	5	32
4 D	11	5	6	8	3	14
5 D	16	6	10	13	3	16
2^{13}C	29	20	9	29	0	30
4^{13}C	20	20	0	19	1	29
5^{13}C	9	6	3	8	1	18
1^{15}N	37	32	0	32	5	35
3^{15}N	34	34	0	29	5	37
1,2 di D	60	30	30	51	9	17

* The computer programme ASFIP was kindly provided by Dr. P. Nösberger and Professor A. Bauder of E.T.H., Zürich [5].

Table 2. Rotational and centrifugal distortion constants for imidazoles (A, B and C in MHz, τ^* values in kHz) and inertial defects (uÅ^2, conversion factor 505376 MHz uÅ^2); s = standard deviation (MHz) in least squares fitting of line-frequencies; τ^*_{aabb} assumed zero in all cases.

Molecule	A	B	C	τ^*_{aaaa}	τ^*_{bbbb}	τ^*_{abab}	$I_C - I_A - I_B$	s
Parent	9725.326 (12)	9374.011 (12)	4771.928 (12)	−13.217 (54)	−13.947 (48)	−6.780 (24)	0.02865 (26)	0.22
1-D	9668.881 (20)	8699.529 (18)	4578.384 (18)	−10.39 (85)	− 9.81 (45)	−6.18 (24)	0.02239 (44)	0.20
2-D	9388.993 (26)	8896.784 (26)	4566.963 (24)	−12.78 (38)	−11.97 (27)	−6.14 (10)	0.02833 (62)	0.40
4-D	9486.409 (48)	8778.562 (36)	4558.162 (26)	−11.7 (2.5)	−13.0 (1.1)	−6.72 (56)	0.02973 (74)	0.05
5-D	9586.929 (42)	8684.701 (30)	4555.635 (20)	− 9.4 (3.3)	−11.0 (1.7)	−4.66 (72)	0.02763 (58)	0.11
1-^{15}N	9695.278 (26)	9188.170 (26)	4716.172 (22)	−13.73 (61)	−13.63 (51)	−6.93 (28)	0.02919 (56)	0.43
3-^{15}N	9721.546 (22)	9135.778 (22)	4708.472 (18)	−14.20 (75)	−14.53 (75)	−7.14 (41)	0.02986 (46)	0.26
2-^{13}C	9522.309 (62)	9354.007 (62)	4717.455 (62)	−11.96 (14)	−13.77 (13)	−6.153 (56)	[a]	0.37
4-^{13}C	9573.922 (60)	9286.009 (60)	4712.609 (56)	−14.68 (62)	−13.96 (70)	−6.70 (43)	0.0290 (14)	0.17
5-^{13}C	9632.227 (74)	9225.537 (62)	4710.987 (54)	−12.74 (79)	−13.63 (62)	−6.69 (28)	0.0287 (13)	0.09
1,2-D_2 [b]	8941.68 (20)	8631.60 (20)	4390.68 (20)	—	—	—	0.033 (6)	—

[a] Inertial defect assumed same as for the parent molecule. [b] Rigid-rotor fit only.

only rotational constants A, B, and C were fitted for this species, and these were not used in the r_s-structure derivation.

IV. Nuclear Quadrupole Coupling Analysis

The ^{14}N-nuclear quadrupole splittings for the mono-^{15}N-imidazoles, including the resolved triplet splittings of the $1_{0,1} \leftarrow 0_{00}$ transitions, were analysed by standard methods. The patterns for three transitions with $J < 3$, for each of these species, were analysed for the best overall fit of coupling constants by means of computer programme H14B*. For the more general case of the di-^{14}N-species, the fitting of the more complex patterns was carried out by means of a further Tübingen programme, ANP1, developed by Dr. H. Günther. Analyses by these methods were carried out for a total of 20 rotational transitions of five isotopic species.

The derived nuclear quadrupole coupling constants in the inertial axes are presented in Table 3, columns a; the numbers in parenthesis are two standard errors in the last figures quoted. Although, for the parent molecule and 1-deuteroimidazole, data based on more highly resolved splittings [6] (Table 3, columns b) have been published, the present results, with the resolution normal for such a molecule in a Stark-modulated spectrometer with an absorption cell in X-band waveguide, allow coupling constants to be compared over a wider range of principal axis directions, and, in particular, for the two mono-^{15}N-species in which the patterns are greatly simplified.

The data in columns a of Table 3 were first treated by taking each isotopic form in turn, in conjunction with the parent form, and the angle of rotation (φ) of the principal axes on isotopic substitution, to derive in each case the off-diagonal term χ_{ab} for the parent species. The orientation of the principal axes of each ^{14}N-nuclear coupling tensor with respect to the principal inertial axes of the parent may then be given in each case by stating the angles (ψ_1 and ψ_3, according to the ring positions) between the A-axis of the parent and the x-principal axis (N at position 1) or z-principal axis (N at position 3) of the respective coupling tensors. An anti-clockwise rotation, under 90°, in going from the A-axis to the tensor axis is treated as positive. The χ_{ab}, ψ_1 and ψ_3 values obtained by such means are included in Table 3. All our data in Table 3 were then treated by a least squares fitting procedure to give the best values of the principal elements and axial orientations of both quadrupole tensors; these are given in Table 4, where the figures in parenthesis again represent two standard errors. This fitting was facilitated by the use of a computer programme, VT23**.

* Developed by Dr. G. Herberich.

** Developed by Dr. V. Typke.

Table 3. Nuclear quadrupole coupling constants for ^{14}N(1) and ^{14}N(3) in imidazole. The angle ψ_1 is that between the tensor x-axis at N(1) and the A-axis of the parent form; ψ_3 is the angle between the tensor z-axis at N(3) and the A-axis of the parent form (see text). The angle φ is that between the A-axis of the given species and the A-axis in the parent (see Figure 1).

	Parent		1-D		2-D	1-^{15}N	3-^{15}N
	(a)	(b)	(a)	(b)	(a)	(a)	(a)
χ_{aa} (1)	1.240 (90)	1.254 (29)	1.411 (101)	1.407 (39)	1.077 (98)		1.198 (50)
χ_{bb} (1)	1.274 (68)	1.283 (37)	1.103	1.146 (42)	1.442 (2)		1.339 (74)
χ_{cc} (1)	−2.514 (112)	−2.537 (47)	− 2.514[a]	− 2.553 (57)	− 2.519 (98)		− 2.537 (48)
χ_{ab} (1) (Parent)	—	—	0.266	0.225	0.383		0.406
ψ_1	—	—	−43.2°	−43.2°	−43.7°		−43.8°
χ_{aa} (3)	−3.955 (46)	−3.952 (24)	− 2.857 (101)	− 2.861 (31)	0.777 (120)	− 3.408 (36)	
χ_{bb} (3)	1.688 (70)	1.694 (36)	0.590	0.676 (41)[b]	− 3.065 (68)	1.149 (60)	
χ_{cc} (3)	2.267 (84)	2.258 (43)	2.267[a]	2.285 (51)[b]	2.288 (138)	2.259 (68)	
χ_{ab} (3) (Parent)	—	—	0.746	0.676	0.966	1.050	
ψ_3	—	—	− 7.4°	− 6.7°	− 9.4°	−10.2°	
φ	0°	0°	19.5°	19.5°	−74.5°	10.2°	− 3.8°

(a) Present work. (b) From reference [6]; error-bounds quoted here are 95% confidence limits.
[a] χ_{cc} fixed at the value for the parent. [b] Laplace relationship is not obeyed.

Table 4. Principal nuclear quadrupole coupling constants (MHz) and their orientations (for definition of ψ_1 and ψ_3 see Table 3; η_1 and η_3 are the asymmetry parameters).

	Microwave		NQR	*Ab initio* calculations		
	(a)	(b)	(c)	(d)	(e)	(f)
χ_{xx} (1)	0.890 (52)	1.043		1.08	1.359	1.290
χ_{yy} (1)	1.633 (58)	1.494		1.31	1.661	1.352
χ_{zz} (1)	− 2.524 (12)	− 2.537	−1.425	− 2.39	−3.020	− 2.641
η_1	0.294 (45)	0.178	0.98	0.093	0.0995	0.0235
ψ_1	−43.7°	−43.2°	—	+22°	—	−50°
χ_{xx} (3)	1.835 (24)	1.774		1.69	1.994	1.927
χ_{yy} (3)	2.278 (24)	2.258		2.03	2.258	1.796
χ_{zz} (3)	− 4.113 (34)	− 4.032	−3.271	− 3.72	−4.252	− 3.723
η_3	0.108 (13)	0.120	0.128	0.093	0.0622	0.0352
ψ_3	− 9.4°	− 6.7°	—	−10°	—	−10°

(a) This work.
(b) Ref. [6].
(c) Ref. [21(b)].
(d) Ref. [18]; split valence shell 4−31 extended basis.
(e) Ref. [24]; double zeta quality.
(f) Ref. [25]; double zeta quality.

Figure 1 shows the orientation of the principal axes of the parent species, and of the tensor axes discussed above. The quadrupole tensor properties given in reference [6] are also listed in Table 4 (column b).

V. Internuclear Distances

The inertial defects of all isotopic species (Table 2) are in accord with a planar structure and hence the atoms can be located in the A/B plane of the parent form with use of changes in I_a and I_b only. The resulting a- and b-coordinates of all atoms, with the exception of the b-coordinate of N(3), are given in Table 5, where the signs follow Figure 1. None of the coordinates is small enough to leave its sign in doubt, and only the a-coordinate of C(2) and the b-coordinate of N(3) are less than 0.3 Å. The acceptability of these small coordinates as derived by the simple substitution method can be checked by using the substitution positions of all atoms to compute the coordinates of the mass-centre, namely: $a_g = -0.0004$ Å and $b_g = -0.0023$ Å. The coordinate a_g is very small and comparable with values found by these methods in similar structures such as pyrrole [7] and pyrazole [2], but the b_g for imidazole is too large to be attributed solely to zero-point vibrational effects. Hence the b-coordinate of N(3) in Table 5 is the adjusted value which conforms with the position of the mass centre. The coordinates are re-expressed as a complete set of r_s-structure parameters in the first column of Table 6. The parameter sets designated as r_s^* and

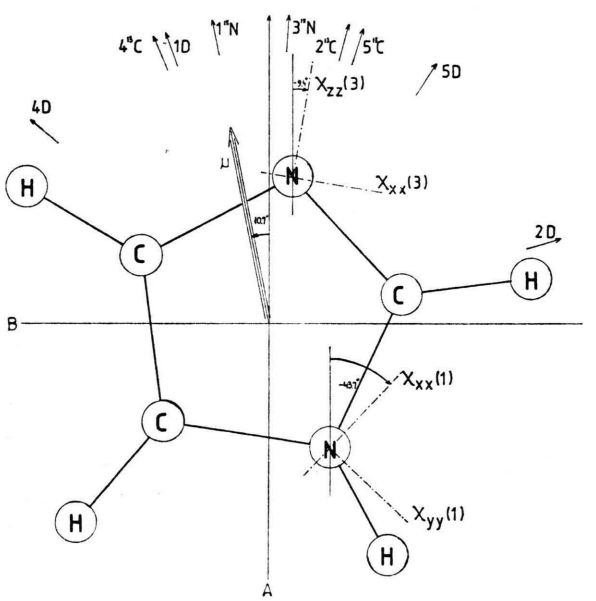

Fig. 1. Structure of imidazole, showing magnitudes and orientations of the dipole moment and principal quadrupole tensor components in the A/B axial system of the parent species. The A-axis directions of isotopically substituted forms are also indicated.

Table 5. Substitution coordinates of atoms in the A/B plane of the parent form of imidazole (Å) (standard errors in parenthesis).

	a	b
H1	1.88643 (23)	0.98108 (10)
H2	− 0.35892 (18)	2.15980 (5)
H4	− 1.09981 (19)	− 1.94886 (10)
H5	1.62882 (23)	− 1.55522 (12)
N1	1.00893 (27)	0.50563 (12)
N3	− 1.18990 (200)	0.19901 *
C2	− 0.22421 (6)	1.08941 (10)
C4	− 0.54652 (13)	− 1.02428 (11)
C5	0.80697 (26)	− 0.85689 (18)

* Adjusted to fit mass-centre condition (see text); the original substitution coordinate is 0.18816 Å.

Table 6. Structural parameters in imidazole (distances in Å, angles in degrees; for angles involving H atoms, see Figure 2).

	r_s	r_s*	r_0*	X-ray		Neutron diffraction	
				(a)	(b)	(c)	(d)
N(1)H(1)	0.9980	0.9950	0.9943	1.048	1.11	1.045	1.053
C(2)H(2)	1.0788	1.0750	1.0747	1.082	1.01	1.077	1.087
C(4)H(4)	1.0775	1.0733	1.0733	0.958	0.98	1.077	1.086
C(5)H(5)	1.0785	1.0766	1.0759	1.031	0.98	1.077	1.087
N(1)C(2)	1.3643	1.3690	1.3704	1.349	1.337	1.347	1.358
C(2)N(3)	1.3135	1.3164	1.3164	1.326	1.311	1.323	1.333
N(3)C(4)	1.3822	1.3880	1.3875	1.378	1.381	1.375	1.389
C(4)C(5)	1.3638	1.3672	1.3676	1.358	1.311	1.368	1.378
C(5)N(1)	1.3774	1.3777	1.3788	1.369	1.373	1.369	1.381
∢N(1)C(2)N(3)	111.99	111.87	111.85	111.3	114.2	111.9	111.8
∢C(2)N(3)C(4)	104.93	105.04	105.08	105.4	102.6	105.1	105.3
∢N(3)C(4)C(5)	110.69	110.45	110.50	109.8	111.2	109.8	109.8
∢C(4)C(5)N(1)	105.48	105.68	105.65	106.3	107.5	106.0	106.0
∢C(5)N(1)C(2)	106.90	106.96	106.93	107.2	104.4	107.1	107.2

(a) Ref. [14], temperature −150 °C. (b) Ref. [15], temperature 20 °C.
(c) Ref. [16], uncorrected at −170 °C. (d) Ref. [16], values corrected to 20 °C. The agreement between the geometry from neutron diffraction and for the gas phase extends also to the angles involving the CH and NH bonds.

r_0^* were calculated as checks by means of the GEOM programme [8], which performs a least squares fitting of structural parameters to all the moments of inertia and to their differences. For the r_0^*-set, moments and differences of moments were given equal weight, while for the r_s^*-set the differences were given ten times as much weight as the moments themselves. It is seen that the r_s^*-figures are very close to those obtained by the ordinary r_s-method with adjustment of the b-coordinate of N(3).

VI. Dipole Moment

This moment was determined in magnitude and line of action from Stark-effect measurements on the normal and 1-deutero species. Static voltages were applied to the Stark electrode, with the addition of a small 100 kHz square wave voltage sufficient to modulate the field-displaced components. The field strength was calibrated in the usual way by measurements, under the same cell conditions, of the Stark displacements of the $J = 2 \leftarrow 1$ transition of OCS, for which the dipole moment was taken as 0.71521 D [9]. The measurements were made with a cell temperature of 57 °C, under conditions such that nuclear quadrupole splittings were largely unresolved. Displacements up to 20 MHz of the following components were measured with field strength up to 1200 Vcm^{-1}:

parent species:

$2_{0,2} \leftarrow 1_{0,1}$ $M = 0$, $M = 1$
$2_{1,2} \leftarrow 1_{1,1}$ $M = 0$
$3_{0,3} \leftarrow 2_{0,2}$ $M = 1$, $M = 2$

1-deuteroimidazole:

$2_{1,2} \leftarrow 1_{0,1}$ $M = 1$
$3_{1,3} \leftarrow 2_{1,2}$ $M = 0$.

For these selected components, the Stark effects were found to be accurately of second order and the displacements such that reasonably precise values of both μ_a and μ_b could be obtained from combinations of the relationships between frequency displacements and the square of the field derived in the usual way by the method of Golden and Wilson [10]. The measurements did not justify consideration of fourth order effects in the Stark displacements, such as were found for pyrazole [11], a highly oblate rotor with large dipole components in both A- and B-axes. Such effects were not apparent. They would be expected to be less important for imidazole than for pyrazole, imidazole being considerably further from the oblate symmetric-top limit than pyrazole, so that the levels responsible for such corrections are less nearly degenerate in imidazole; the effects would also be lessened by the fact that μ_b is quite small in imidazole.

By the overall fitting of the measurements, the following information is obtained:

	parent molecule	1-deuteroimidazole
μ_a	3.603 ± 0.03 D	3.64 ± 0.05 D
μ_b	0.680 ± 0.03 D	0.64 ± 0.05 D
μ (total)	3.667 ± 0.05 D	3.70 ± 0.10 D

The components for the parent molecule show that the line of action of the dipole moment makes an angle of 10.7 (5)° with the A-axis. The changes in dipole components on deuteration leave little doubt that the line of action of the total moment is as indicated in Figure 1. This is consistent with the relative strengths of the a- and b-type spectra found for the various isotopic species.

VII. Discussion

a) Structure

Figures 1 and 2 illustrate the occurrence in imidazole of the effect noted in several similar systems [1] whereby the CH bond directions lie off the bisectors of the external ring angles, towards an adjacent hetero atom. This effect is seen in the CH bonds at the 4- and 5-positions, but not greatly in that at the 2-position, which lies between two hetero atoms. The ring angle at the pyridine-type nitrogen is lower than at the carbons, as has been found in pyrazole [2], oxazole [12] and other cases [1], and is perhaps explained as due to greater p-character in the N-orbitals used for ring bonding than in the corresponding orbitals centred on carbon [13]. Figure 2 allows more detailed comparisons with the complete structures of pyrrole, pyrazole and oxazole. The ring bonds in imidazole do not differ dramatically from those in oxazole, although variations of 0.01 — 0.02 Å occur. Whereas pyrazole differs from pyrrole chiefly in the region of the N–N bond, the changes on passing from pyrrole to imidazole largely involve the three bonds from positions (2) to (5). When allowance is made for the differences in covalent radii of N and C in this comparison, the insertion of N(3) in imidazole appears to be accompanied by a shortening of the bonds N(3)–C(2) and C(4)–C(5), with a lengthening of N(3)–C(4). This suggests some lowering of aromatic character in imidazole relative to pyrrole.

The comparison in Table 6 with results of X-ray and neutron diffraction results shows that the C_3N_2 ring structure is largely retained on passing from the gaseous to the solid state, except that the ring bonds at N(1) are perhaps somewhat shortened and C(2)–N(3) elongated in this process. This must be an effect of hydrogen bonding, which is strongly supported by the greater length of N–H in the solid. This difference is made particularly clear by the

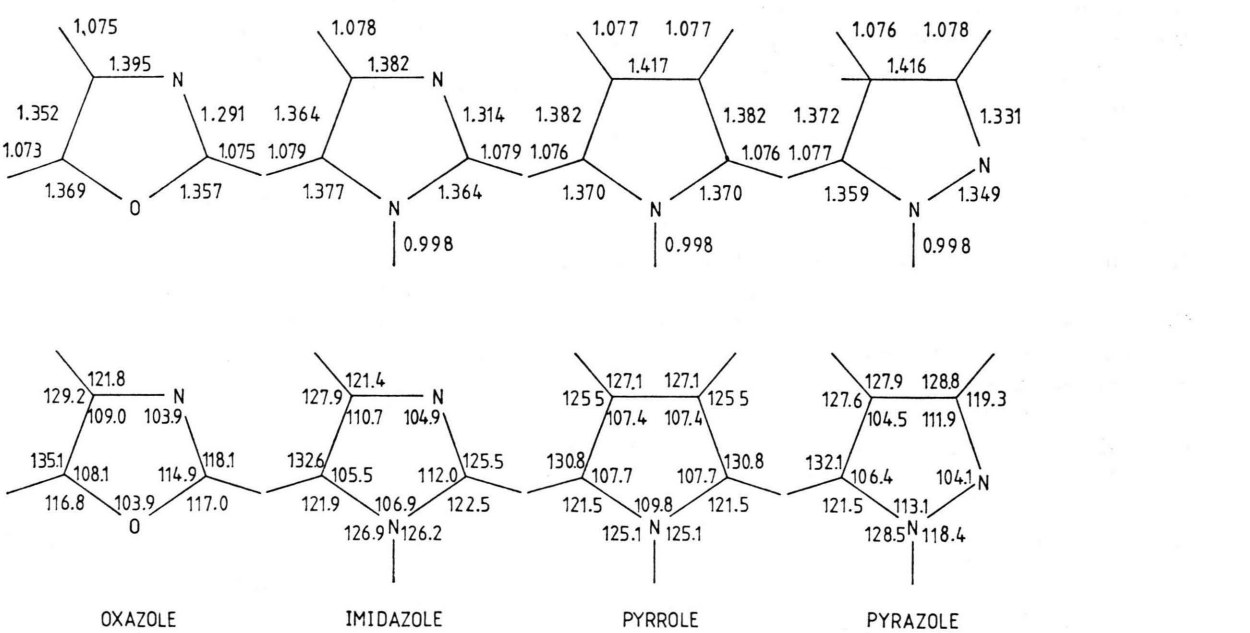

Fig. 2. A comparison of the structures of imidazole, pyrrole, oxazole and pyrazole.

neutron diffraction results, where the C–H distances are close to those in the gas phase, but N–H is 0.05 Å longer.

b) Electron Distribution

The dipole moment vector in gaseous imidazole agrees closely with general expectations; for example, the magnitude and direction of the total moment is close to that obtained by combining the moment of pyrrole (taken as $\overleftarrow{N-H}$) with that of pyridine (operating along the external ring angle bisector at position (3) in the sense $\gtrless N: \mapsto$). Such considerations leave no doubt that the sign of μ corresponds to negative charge displaced in the arrowed direction in Figure 1.

The moment of imidazole in benzene extrapolated to infinite dilution, 3.8 D [17] also agrees very well with our results, as do theoretical calculations of the moment by O'Konski and Jost [18].

The ^{14}N-nuclear quadrupole coupling tensors bear considerable resemblance to those in pyrrole [19] (for position 1) and in oxazole [20] (for position 3). The electron population analysis given for N(3) in oxazole [20] could be carried through with comparable findings in the imidazole case. Discussion of the gas-phase tensors has already been given [6] in relation to the spectra studied in higher resolution, although in this there is perhaps one aspect which requires further clarification, arising from the fact that the figures there given for N(3) in 1-deuteroimidazole (Table 3, column b) do not fulfil the Laplace relationship. It is not clear how the consequent uncertainties, coupled with the need to keep χ_{cc} invariant, may affect the best values of the tensor orientation expressed in the angle ψ_3.

The convincing findings of Edmonds [21] for NQR measurements on imidazole are included in Table 4. The differences between these data and those for the gaseous state are of the expected order. For position (3), the differences in coupling constants for the gas and for the solid resemble those observed for ammonia [22]. For the pyrrole-type nitrogen, however, the differences are appreciably larger. Here, the principal coupling constant for the solid, which we have assumed to remain perpendicular to the molecular plane, has only some 44% of its value in the gas phase, while the dramatic change in asymmetry parameter on solidification shows that one of the coupling constants in the molecular plane has become very small. That these changes are indeed consistent with hydrogen bonding between the N(1) of one molecule and N(3) of a second is well shown by consideration of NQR findings for 1,2-dimethylimidazole, in which no such hydrogen bonding can occur [23]. For this molecule, the coupling constant found for N(1) is -2.4084 MHz, with an asymmetry parameter of 0.199, while the constant for N(3) is -3.5267 MHz, with an asymmetry parameter of 0.102. These figures are quite close to those for gaseous imidazole. We conclude therefore that, in imidazole, the hydrogen bonding strongly influences the field gradient at the nitrogen to which the involved hydrogen is principally bonded, and only to a much lesser extent the field gradient at the nitrogen to which the hydrogen bonding is established.

Table 4 also shows the results of more recent *ab initio* molecular orbital calculations of the nuclear quadrupole tensors in the free imidazole molecule [18, 24, 25]. Apart from the χ-values, such work also now includes computed directions of the principal tensor axes, which form a critical test of the theoretical treatment. While variations between results of different approaches are clear, there is, overall, an encouraging degree of agreement with the experimental findings.

Acknowledgement

We are grateful to Professor J. H. Ridd for a gift of the sample of 2-deuteroimidazole, to Dr. P. Nösberger, Dr. H. Günther, Dr. G. Herberich, and Dr. V. Typke for assistance with computer programmes, and to the Science Research Council for a Research Studentship (to J.G.) and support through a Research Grant. D.C. thanks the Leverhulme Trust and the University College of North Wales for post-doctoral fellowships during the tenure of which this work was partly performed.

[1] J. Sheridan in "Physical Methods in Heterocyclic Chemistry" (ed. A. R. Katritzky), Vol. VI, Academic Press, New York 1974, p. 53.
[2] L. Nygaard, D. Christen, J. T. Nielsen, E. J. Pedersen, O. Snerling, E. Vestergaard, and G. O. Sørensen, J. Mol. Struct. **22**, 401 (1974).
[3] R. Behrend and J. Schmitz, Ann. Chem. **277**, 337 (1893).
[4] A.-M. Bellocq, C. Perchard, A. Novak, and M.-L. Josien, J. Chim. Phys. **62**, 1334 (1965).
[5] P. Nösberger, A. Bauder, and Hs. H. Günthard, Chem. Phys. **1**, 426 (1973).

[6] G. L. Blackman, R. D. Brown, F. P. Burden, and I. R. Elsum, J. Mol. Spectrosc. **60**, 63 (1976).
[7] L. Nygaard, J. T. Nielsen, J. Kirchheimer, G. Maltesen, J. Rastrup-Andersen, and G. O. Sørensen, J. Mol. Struct. **20**, 119 (1969).
[8] P. Nösberger, A. Bauder, and Hs. H. Günthard, Chem. Phys. **1**, 418 (1973).
[9] J. S. Muenter, J. Chem. Phys. **48**, 4544 (1968).
[10] S. Golden and E. B. Wilson, J. Chem. Phys. **16**, 669 (1948).
[11] W. H. Kirchhoff, J. Amer. Chem. Soc. **89**, 1312, 2242 (1967).
[12] A. Kumar, J. Sheridan, and O. L. Stiefvater, Z. Naturforsch. **33a**, 145 (1978).
[13] L. Pauling, The Nature of the Chemical Bond, 3rd ed., Cornell Univ. Press, New York 1960, p. 140.
[14] S. Martinez-Carrera, Acta Cryst. **20**, 783 (1966).
[15] G. Will, Z. Kristallogr. **129**, 211 (1969).
[16] R. K. McMullan, J. Epstein, J. R. Ruble, and B. M. Craven, Acta Cryst. **B35**, 688 (1979).
[17] K. Hofmann, Imidazole and its Derivatives, Vol. 1, Interscience, New York 1953.
[18] C. T. O'Konski and J. W. Jost, J. Mol. Struct. **58**, 475 (1980).
[19] K. Bolton and R. D. Brown, Aust. J. Phys. **27**, 143 (1974).
[20] A. Kumar, J. Sheridan, and O. L. Stiefvater, Z. Naturforsch. **33a**, 549 (1978).
[21] (a) D. T. Edmonds and P. A. Speight, J. Mag. Res. **6**, 265 (1972); **9**, 66 (1973). (b) M. J. Hunt, A. L. Mackay, and D. T. Edmonds, Chem. Phys. Lett. **34**, 473 (1975).
[22] (a) S. S. Lehrer and C. T. O'Konski, J. Chem. Phys. **43**, 1941 (1965). — (b) T.-K. Ha and C. T. O'Konski, J. Chem. Phys. **51**, 460 (1969).
[23] E. Schempp, private communication.
[24] T.-K. Ha, Chem. Phys. Lett. **37**, 315 (1976).
[25] M. H. Palmer, I. Simpson, and R. H. Findlay, Z. Naturforsch. **36a**, 34 (1981).